Journal Home Page: https://sjes.univsul.edu.iq/

Research Article:

Experimental Investigation on Flexural Strengthening of Reinforced Concrete Beams with Opening Using Heavy-Duty Metal Straps

Omer Mahmood Haji Ahmed [1,a,*]
Wrya Abdullah [2.a]
[a] University of Sulaimani ,College of Engineering, Civil Engineering Department, KR, Iraq

Article Information

Article History:
Received: September 18th , 2025
Accepted: January 22, 2026
Available online: April , 2026

Keywords:
Beams , Opening Shape , Strengthening Methods , Strengthening Material

About the Authors:

Corresponding author:
Omer Mahmood Haji Ahmed
Email: omer.haji@univsul.edu.iq

Researcher Involved:
Assist. Prof. Dr Wrya Abdullah
Email: wrya.faraj@univsul.edu.iq

DOI https://doi.org/10.17656/sjes.10199

Abstract

Beam openings have been proven to reduce beam strength; therefore, Strengthening is necessary to enhance the beam's load capacity, failure mode, ductility and first cracking load. This strengthening can be carried out using internal steel rebar and FRP; however, the use of metal straps has never been tested. Therefore, this study examines the application of heavy-duty metal straps (HDMS) to enhance the strength of RC beams with openings. For this purpose, seven reinforced concrete (RC) beams were tested, each with a depth of 250 mm, a width of 150 mm, and a clear span of 1200 mm. Six beams had an opening in the mid-span, and one was a solid control specimen. The shape of the opening (circular and square) and the method of HDMS application (vertically and horizontally) were the main parameters. The openings had equivalent areas, utilizing 110 mm diameter circular openings and 100 mm × 100 mm square openings. Horizontal HDMS around circular and square openings increased the load-carrying capacity of the beams by 10% and 16%, respectively, compared to the solid control beam. In contrast, the vertical HDMS around the opening increased the first cracking load of the specimens by 16% and 5% for circular and square openings, respectively, compared to the unstrengthened control beams with openings.

1. Introduction

Even though beams are susceptible to damage during earthquakes, openings in them have become unavoidable to house various services, including gas, electricity, water supply, and sewage [1, 2]. Also, to accommodate essential building services, including ductwork, electrical and telecommunication cabling, plumbing and sewage networks, structural engineering must integrate these penetrations into the initial design phase to ensure structural integrity [1-5]. Additionally, the height constraints set by the mechanical and architectural engineers lead to openings in RC beams of a building. Figure 1 illustrates RC beams with web openings. These openings may aggravate the situation of the beams, which are used in the frame-building method to transfer lateral loads during earthquakes, which occur frequently in various parts of the world. Because openings reduce the stiffness and capacity of the beam and increase the size of deflection cracks. Additionally, the higher stress concentration at the opening chords, particularly at the opening corners, causes the beam's behavior to shift from simple to complex [3]. Hence, to enhance its load-bearing capacity, the beam could be reinforced, thereby extending its structural service life [4]. Furthermore, it is shown that adding openings to existing beams and their circular shapes significantly increases their vertical deflection while reducing their flexural strength, excessive cracking, excessive bending, and decreased stiffness [5-8]. The amount of these adverse influences of openings can be related to the size of the opening. An opening is classified as "small" if it is sufficiently small to preserve beam-type behavior or if standard beam theory remains applicable; conversely, large openings are those that exhibit the failure of frame-type or Vierendeel behavior [9]. To quantify the measurement of the size of the opening, the following measures can be used. For square and rectangular openings, if $d \leq 0.25\ h$ (where d is the opening depth and h is the beam height), they are classified as small; otherwise, they are categorized as large [9-11]. Additionally, for circular openings, if the diameter exceeds 40% of the web's depth,

the opening is considered large [13-15].

Various techniques for strengthening and analyzing RC beams with openings have been presented, and numerous studies have been conducted to predict their load–deflection response, cracking behavior, and ultimate performance [16-18]. Strengthening methods include internal steel reinforcement and external FRP applications. It is proven that strengthening the chords of an opening internally and externally increases the capacity of the beams [19]. Furthermore, utilizing carbon-fiber-reinforced polymer (CFRP) sheets or steel plates for external strengthening is often more efficient than utilizing steel for internal reinforcement [20]. The effect of the dimension of the openings has been studied widely in the literature. Mondal et al. [21] tested eleven beams: one solid beam and ten beams with openings with varying dimensions, focusing on strengthening and rehabilitation. The findings indicate that the opening dimensions are a critical determinant of the reduction in first cracking load. Additionally, when openings are large, they control the beam's performance to the extent that FRP strengthening becomes ineffective in increasing the total load-carrying capacity. FRP can fail via two primary mechanisms: rupture or debonding from the concrete surface. To prevent debonding and premature beam failure, FRP is typically wrapped around the opening at a minimum distance of 80 mm from the edge [21].

Moreover, three different CFRP strengthening configurations were evaluated by Akhila and Arathi [22]: CFRP inside the opening, CFRP around the opening, and a combination of both. The combined application (inside and around) proved more effective than reinforcement placed solely inside the opening [22]. Additionally, RC beams with wide openings can be strengthened using externally bonded CFRP laminates [23]. Researchers noted that a large central opening reduced beam capacity by 50%, but the application of CFRP laminates subsequently increased strength by 80–90% [23].

Other methods of strengthening have been used, such as using glass fiber–reinforced polymer (GFRP). Miruthun, G. et al. [24] studied nine specimens with dimensions depth 250 mm, width 150 mm, and total span 2000 mm. The results demonstrated that the intermittent GFRP wrapping proved more effective than other methods, yielding higher strength and ductility with lower deflection. This specific application pattern significantly strengthens cracked RC beams, providing a substantial boost to their overall load-bearing capacity and resilience. The specimens with relatively large openings showed that failure behavior was governed primarily by opening size. In these cases, GFRP did not significantly enhance ultimate load-carrying capacity or alter the failure mode [24]. Additionally, it is proven that even drilled openings will have significant adverse behavior of the RC beams. Amer [25] investigated the impact of in-situ drilled rectangular and circular openings on the flexural behavior of eight case-in-place RC beam specimens. Results indicated that drilling openings, regardless of shape, reduce flexural strength and significantly increase vertical deflection.

A relatively recent and cost-effective method for reinforcing structural members, particularly beams, is the use of metal straps. This approach is considered inexpensive and simpler to implement than alternative methods such as FRP, concrete caging, steel caging, or ferrocement.

Metal straps are composed of ultra-high-strength, flexible steel with a tensile yield strength exceeding 900 MPa. This material is available in long strips with a variety of widths and thicknesses [26].

The literature includes many investigations into the practical and theoretical applications of the material for various structural members [27–40]. Some of this research has been limited to small-scale specimens, such as 100 mm x 100 mm prisms or standard 150 mm x 300 mm concrete cylinders. However, one published study [41] examined the strengthening of beams using metal straps. RC beam specimens were fabricated with a total length of 1200 mm and a rectangular cross-section of 150 mm × 200 mm. The beam geometry was intended to simulate a flexural member with a known lap splice length. The primary bottom flexural reinforcement consisted of two steel bars with diameters of 12 mm and 16 mm, joined at the midspan zone. Each beam had two 50 mm × 100 mm notches at the bottom to define the lap length and expose the primary flexural reinforcement for measurement. Two continuous 10 mm bars constituted the top reinforcement. Outside the spliced zone, 6 mm fully closed plain stirrups were placed at 100 mm intervals to prevent shear failure, with no openings present.

Conversely, to this date, a paucity of literature regarding the application of metal straps for the structural enhancement of RC beams with openings, particularly concerning their performance in either the flexural or shear zones.

The primary purpose of this material is to promote confinement, which is beneficial for high-strength thin columns, beams that fail in shear, and short columns subjected to lateral stresses. However, one difficulty in its effective use for beams that fail in flexure is that relatively few researchers have investigated this application [42]. This study focuses on using a metal strap because it offers a more efficient application process and a lower cost profile, while avoiding the technical disadvantages associated with traditional strengthening methods.

2. Objective:

This study investigates the structural behavior of RC beams with openings strengthened with HDMS. It presents experimental results detailing the impacts of these openings on load-bearing capacity, failure mechanism, crack propagation, and mid-span deflection,

as well as the first cracking load. Additionally, the research evaluates the efficacy of horizontal and vertical HDMS applications in strengthening circular and square openings within beams of geometric dimensions.

3. Material and Research Methods:

3.1. Materials:

In this study, the following materials were used. First, the HDMS measured precisely 31.75 mm in width and 0.8 mm in thickness. The tensile strength of the metal straps was found to be 928 MPa on average, and their modulus of elasticity was 237 GPa. The steel reinforced bars had a maximum elongation capacity of 14.6%, and their average yield and tensile strengths were 602 and 787.2 MPa, respectively. For the mix design of the concrete, the guidelines of ACI-C211.1 (1991) [43] were used. The concrete's target cylindrical compressive strength (f'_c) was established to be 28 MPa. The properties of the concrete ingredients were as follows: The OPC type of cement was used as the binder for the mix. Furthermore, 12.5 mm was the largest size of coarse aggregate. The moisture content of coarse aggregate was 0.4%, while that of fine aggregate was 0.6%. The coarse aggregate's absorption rate was 0.81%, whereas the fine aggregate recorded 1.55%. The fine aggregate's fineness modulus was 3.25. The coarse and the fine aggregates complied with ASTM C33 (2018) [44]. The mix ratio of cement, sand, gravel, and water employed in this study was 1:2.36:2.06:0.48, respectively. Plywood was used to construct the beam formwork for the concrete casting. The plywood forms were cleaned and lubricated before casting. To guarantee the appropriate concrete cover thickness, it is important to note that 25 mm bolsters were utilised as the concrete cover. Upon completion of the formwork preparation, the reinforcement cages were positioned within the moulds. Subsequently, the concrete was cast and consolidated using a needle vibrator to ensure adequate compaction. To guarantee adequate consolidation, the concrete was poured into the beam in 125 mm layers and compacted after each layer. Lastly, a spatula was used to level and smooth the beams' upper surfaces. Figure 2 shows the stages of preparation and casting concrete of the specimens. Three-cylinder moulds with a diameter of 150 mm and a height of 300 mm were obtained during the casting process to test the concrete's compressive strength. After that, the beam specimens underwent a 28-day curing process. Following the curing phase, the specimens' testing faces were painted white. A concrete angle grinder was used to grind the beam's surface and the point of contact with the testing apparatus to prepare the specimens for testing and provide a level surface for the loading jacks.

3.2. Details of the Beam Specimens:

A total of seven RC beams were cast. Each beam featured a clear span of 1200 mm and a cross-section of 150 mm x 250 mm (width x depth), with a 25 mm concrete cover provided for the longitudinal and transverse reinforcement. Shear reinforcement consists of 10 mm diameter stirrups spaced at d/2 = 100 mm (where d represents the effective depth). Both the tension and compression reinforcement comprised two 10 mm diameter longitudinal bars. Figure 3 illustrates the beam configuration, cross-sectional details, and loading locations. An LVDT was positioned at the mid-span to monitor vertical deflection. The specimen nomenclature is detailed in Figure 4. As shown in Figure 5(a), beam CS serves as the solid control specimen without opening and without strengthening. Figures 5(b) and 5(c) present beams CFCO and CFSO, which contain circular and square openings at mid-span, respectively. These similar configurations were further evaluated using HDMS strengthening: two specimens with circular and square openings were strengthened vertically on each face, as in Figures 5(d) and 5(e) (SFCOV and SFSOV), respectively, while two specimens also with circular and square openings were strengthened horizontally, as in Figures 5(f) and 5(g) (SFCOH and SFSOH), respectively. All specimens maintained identical dimensions and reinforcement ratios. For specimens with circular openings (CFCO, SFCOV, and SFCOH), the diameter of the openings was 110 mm, and classified as 'large,' given that the opening-to-beam height ratio is 0.44. Similarly, for specimens with square openings (CFSO, SFSOV, and SFSOH), the dimensions of the openings were 100 mm × 100 mm, and classified as 'large,' with a ratio of opening to beam height of 0.4 [19, 22].

3.3. Beam strengthening:

The strengthening of the beam specimens was carried out using HDMS, which is shown in Figure 6(a). The application of the HDMS was carried out using bolts and nuts with washers, as in Figure 6(b). There are two methods of strengthening with HDMS: vertically and horizontally. The vertical strengthening begins above the specimen, descends from one side of the opening, passes beneath the specimen, and then continues along two sides of the opening until it reaches the top of the specimen. Each strap measures 750 mm in length, as in Figure 7(a). In horizontal strengthening, a 650 mm length of strip was used, with four strips applied to two faces of the specimen and fixed above and below the opening. It was done with eight bolts and nuts, as shown in Figure 7(b). The bolt size was φ10 mm with a length of 100 mm, and the nut size was φ17 mm to tighten the bolt to a very tight fit in the specimen. This study's limitations include the limited sample size regarding the specimen's length and cross-section, the absence of a slab section with a beam cross-section, the reliance on a single bolt size for tightening, and the use only of normal-strength concrete in the mixing process.

4. Results and Discussion

4.1. Concrete Compressive Strength:

The average compressive strength of the three concrete cylinders was 27.31 MPa, while the target strength of the concrete mixture was 28 MPa. Table 1 lists the specific

characteristics of each cylinder.

4.2. Beams results

The results of the experimental study are presented for each specimen. A summary of the characteristics defining each evaluated beam's behavior is given in Table 2. The results of the control beams and the strengthened beams are compared, and they are analysed and discussed in the following sections.

4.2.1 Cracking behavior and mode of failure:

All experimental specimens exhibited a flexure failure mode, with recorded strains on the longitudinal reinforcement exceeding 0.5%, which is greater than the tensile strain of the reinforcement in the tension zone. This indicates that the flexure failure of the tension steel occurred. In the control beam (CS), crack initiation occurred within the tension zone, with cracks propagating vertically toward the neutral axis. These flexure cracks widened progressively until failure, as illustrated in Figure 8(a); no abrupt shear failure or localized crushing at the loading points was observed.

In comparison to the solid control beam, the initial cracking loads for specimens with openings were approximately equal. This is attributed to the fact that the opening heights remained outside the primary compression zone of the beam section. For circular openings, as in Figure 8(b), cracks initiated at the center below the opening, whereas for square openings, as in Figure 8(c), cracks initiated below the specimen towards the corner of the opening due to stress concentration in the opening corners.

Notably, vertical strengthening significantly delayed the onset of cracking. Specifically, the first cracking load increased by 43% for circular openings and 64% for square openings compared to unstrengthened beams. The resulting crack patterns are presented in Figures 8(d) and 8(e), which represent beam SFCOV and SFSOV, respectively. In specimens with horizontal strengthening, crack formation above the openings was suppressed; the HDMS effectively acted as a crack arrester, intercepting the propagation path and preventing vertical extension through the opening region, as in Figure 8(f) and 8(g) for beam SFCOH and SFSOH, respectively.

4.2.2 Load-deflection diagram:

The behavior of the tested beams—including ultimate carrying capacity, ductility, deflection, first cracking load, and crack width is presented in the following sections.

Effect of the opening:

The results demonstrate that the square opening outperforms the circular opening in terms of ultimate load-carrying capacity, ductility, and deflection for RC beams, despite the slight difference in ultimate load between the two shapes of the opening in the RC beams. Still, the difference in ductility and deflection has been clearly shown, as in Figure 9. Compared to the CS, CFCO and CFSO, ultimate loads were 2% and 1% lower. The slight variation between CS, CFCO, and CFSO in ultimate load is attributed to the small compression block located outside the opening. Although the severe stress concentration inherent to square openings triggers premature yielding in CFSO reinforcement compared to CS and CFCO configurations, the specimens ultimately exhibit comparable peak load capacities. This suggests that post-yield redundancy and internal force redistribution effectively mitigate the early localized distress, allowing the members to achieve a normalized ultimate strength. Compared to the CS and CFSO, CFCO's deflection and ductility were greatly reduced by the circular opening in the specimen, because the applied load on the CFCO did not reach the final deflection, as seen in Figure 10. The allowable deflection, according to the ACI 318-25 [45] serviceability equations, is $\frac{L}{240}$ (where L is the clear span between two supports of the RC beam). Figure 10 shows how the opening shape affects the load-deflection relationships at a time when both openings had the same area, but the circular opening height was relatively higher than the square opening height. This is another reason for the reduced ductility and deflection of the specimen with a circular opening [19, 22].

Effect of the vertical strengthening:

Vertical strengthening increased the specimens' ductility, deflection, and load-carrying capacity for both square and circular openings, as in Figure 11. Figure 12 shows the impact of vertical strengthening. Comparing SFCOV with CFCO, SFCOV was strengthened vertically with HDMS and the flexural resistance increased by 5%, ductility increased by 33%, and deflection increased by 25% compared with CFCO.

On the other hand, the testing of specimens CS, CFSO, and SFSOV, as shown in Figure 13, indicates the impact of vertical strengthening on their behavior. SFSOV specimens enhanced flexural resistance, ductility, and deflection by 6%, 34%, and 77%, respectively, compared with CFSO. Even though the deflection of SFSOV was greater than that of SFCOV, the ductility of both circular and square openings increased by 33% compared to their controls. Compared to the CS, the SFCOV specimen showed a 3% increase in ultimate load-carrying capacity, but experienced significant decreases in ductility and deflection by 28% and 46%, respectively. In contrast, the SFSOV specimen demonstrated improvements across all metrics: its ultimate load capacity rose by 5%, ductility by 3%, and deflection by a substantial 88%.The lower deflection recorded for the SFCOV (9.0 mm) compared to the SFSOV (31.6 mm) is attributed to the fact that the SFCOV did not reach its final deflection under the applied load; however, it still exceeded the allowable deflection limit of 5 mm. A significant finding of this study is that vertical strengthening is more effective for specimens with square openings than those with circular openings. This is because the strengthening prevented early inclined cracks from forming at the sharp corners of the square openings. Furthermore, the square opening

specimens benefited from a smaller opening height to specimen depth ratio relative to the circular specimens [19,22], ultimately leading to higher ultimate loads, greater deflection, and a large area under the load deflection curve for the SFSOV.

Effect of the horizontal strengthening:

Horizontal strengthening increased the load-carrying capacity and deflection for both square and circular openings; however, a ductility increase was observed only for the square opening, as in Figure 14. Figure 15 shows the impact of horizontal strengthening. Comparing SFCOH with CFCO, SFCOH was strengthened horizontally with HDMS and the flexural resistance increased by 12%, ductility decreased by 26%, and deflection increased by 63% compared with CFCO. On the other hand, the testing of specimens CS, CFSO, and SFSOH, as shown in Figure 16, indicates the impact of vertical strengthening on their behavior. SFSOV specimens enhanced flexural resistance, ductility, and deflection by 17%, 83%, and 55%, respectively, compared with CFSO. For SFCOH, the HDMS's interference with the reinforcement caused a delay in yielding, which reduced ductility, as seen in Figure 15. In contrast, for SFSOH, stress concentrations at the corners of the control specimen (CFSO) resulted in lower ductility in the control specimen with opening and higher ductility in the strengthened specimen, as in Figure 16. At the same time, other properties of the strengthened specimens improved compared to the unstrengthened control specimens. The SFCOH specimen's load-carrying capacity, ductility, and deflection increased by 10%, decreased by 60%, and decreased by 30%, respectively, compared to CS. Meanwhile, SFSOH showed increases of 16%, 41%, and 65% in load-carrying capacity, ductility, and deflection, respectively, compared to CS. The interference of HDMS with reinforcement causes SFCOH's ductility to decrease by 60% relative to CS. All behaviors of specimens with square openings were superior to those with circular openings because the height of the square opening is less than that of the circular opening, despite both having the same area. Horizontal strengthening acts as longitudinal reinforcement, causing the concrete to engage more of its thickness as a compression block and thus increasing the ultimate load-carrying capacity of the strengthened specimen and then its impact on increasing ultimate load is larger than that of vertical strengthening.

4.2.3 First Cracking Load:

Due to the small size of the compression block, the opening did not significantly affect the first cracking load of the specimen with an opening. The first cracking values of all specimens are shown in Figure 17. In contrast to horizontal strengthening, in which the first cracking load appears sooner than in their control beams, vertical strengthening with HDMSs increases the specimen's first cracking load by 16% and 5% for SFCOV and SFSOV, respectively, compared to their controls without strengthening. This is due to the strengthening direction opposing the load direction, making the strengthened concrete in the tension zone more effective than horizontal strengthening.

4.2.4 Crack Width

The maximum crack widths recorded were 11 mm for the CS and SFCOH beams. Conversely, the minimum crack widths were 5 mm for CFCO and 6 mm for CFSO. These lower values were attributed to the presence of unstrengthened openings, which resulted in lower ductility. Comprehensive crack width data are presented in Figure 18. The SFCOV, SFSOV, and SFSOH beams exhibited final mid-span crack widths of 8 mm, 10 mm, and 9 mm, respectively. These relatively lower values are a consequence of the specimens not reaching their ultimate collapse loads, despite their deflections exceeding the code-mandated limit of 5 mm. These findings indicate that crack widths among the control, vertically strengthened, and horizontally strengthened beams vary primarily due to the introduction of openings in the flexure zone. The tested beams with openings strengthened vertically and horizontally are shown in Figure 19, which displays the tested specimens, none of which experienced any bolt pullout or HDMS breakage. In all cases, failure resulted from the yielding of the steel reinforcement and the crushing of the concrete.

5- Analytical part:

In this section, the common theories of RC beams subjected to bending are applied using the equations from ACI 318-25 [45].

Analytical calculation of SFSOH: Compression block and tension forces are illustrated in Figures 20 and 21.

Assumptions:

1- Neglecting top reinforcement.
2- Neglecting self-weight.

A_{ms} = 32 x 0.8 = 25.6 mm².

f'_c = 27.31 MPa.

f_y = 602 MPa.

$Steel\ Elongation$ = 14.5%.

fy_{ms} = 928 MPa.

$HDMS\ Elongation$ = 9%.

$a = \beta 1.C \qquad \beta 1 = 0.85$ (for $f'c = 28$ MPa)

$\emptyset f'c.a.b = A_s x\ f_y + (A_{ms} x\ E_{ms} x \varepsilon_{ms})_{top} + (A_{ms} x\ E_{ms} x \varepsilon_{ms})_{bottom}$

0.85 * 27.31 x a x 150 = 2 x 78.5 x 602 + 25.6 x 237000 x (116 + 1578) x 10^{-6}

a = 30.1 mm.

$Mu = A_s x\ f_y$ x $(d_s - \frac{a}{2})$ + $(A_{ms}$ x E_{ms} x $\varepsilon_{ms})$ x $(d_{ms} - \frac{a}{2})$ + $(\frac{A_{ms}}{2}$ x E_{ms} x $\varepsilon_{ms})$ x $(d_{ms2} - \frac{a}{2})$.

=2 x 78.5 (602) x $(210 - \frac{30.1}{2})$ + 25.6 x 237000 x 0.001578 x $(191 - \frac{30.1}{2})$

+ 25.6 x 237000 x 0.000116 $(59 - \frac{30.1}{2})$ = 20140988.72 N.mm.

$Mu = \frac{P\,X\,L}{4}$

P = $(\frac{20140988.72x\,4}{1200})$ = 67136.63 N = 67.14 kN.

P obtained from the test = 85 kN > 67.14 kN=calculated.

Symbols:

A_{ms} = Area of metal strap section.

d_s= effective depth of reinforcement = 210 mm.

d_{ms} = effective depth of metal strap = 191 mm.

E_{ms} = Modulus of elasticity of metal strap = 237 GPa.

ε_{ms} = Strain of metal strap.

f'_c = compressive strength of concrete.

f_y = yield strength of bar reinforcement.

a = depth of compression block.

b = beam width.

fy_{ms} = yield strength of the metal strap.

As in Table 3, all experimental ultimate loads were slightly higher than the values calculated using ACI 318-25 [45] equations. This demonstrates that the behavior of the tested specimens aligns with the code equations, which typically provide conservative estimates. A significant observation is that the discrepancy between experimental and calculated ultimate loads was greater for strengthened specimens, particularly those with horizontal strengthening, than for unstrengthened ones. This is due to the presence and specific placement of the HDMS, which the standard equations may not fully account for. The superior load resistance of the horizontally strengthened specimens compared to the vertically strengthened ones is directly attributed to the orientation of the reinforcement; horizontal strengthening aligns more effectively with the primary tensile stresses, thereby contributing more significantly to the beam's overall capacity.

4 Conclusion

The following conclusions can be drawn from the study:

1. Openings at the midspan do not significantly weaken the beam unless their height exceeds the depth of the concrete compression block.
2. Vertical strengthening in beams with openings has a greater effect on increasing the first cracking load than horizontal strengthening, with increases of 43% for circular openings and 64% for square openings compared to horizontal strengthening.
3. Vertical strengthening increases the ultimate load-carrying capacity by 3% for circular openings and 5% for square openings compared to solid beams.
4. When compared to an unstrengthened beam with an opening, SFCOV increases the load capacity by 5% and SFSOV increases the load capacity by 6%.
5. Horizontal strengthening increases the ultimate load capacity by 12% and 17% for circular and square openings, respectively, compared to their control beams without strengthening.
6. All beams strengthened with HDMS failed in flexure because their compression blocks were out of the openings in all specimens.
7. The crack width in solid beams and horizontally strengthened beams is 11 mm, which is greater than that in beams with openings (5 mm and 6 mm) and in vertically strengthened beams. This is due to more gradual failure and greater ultimate deflection, indicating higher ductility in the solid and horizontally strengthened beams.
8. For RC beams with openings in the flexure zone, HDMS strengthening horizontally increased the ultimate load-carrying capacity more than that with vertical strengthening, because horizontal strengthening had a higher contribution to flexural resistance, which acts as reinforcement bars due to its direction.
9. For ductility and deflection, the vertical strengthening was more effective than the horizontal strengthening, because the direction of the vertical strengthening led to greater deflection in RC beams.
10. For RC beams with openings in the flexure zone, HDMS strengthening improved the behavior of beams with square openings more than those with circular openings.

The future recommendation

To demonstrate the impacts of HDMS strengthening, it is recommended that high-strength concrete be used with RC beams that contain openings in the future.

References

[1] Zuhair, Mohammad, and Parikshit N. Deshmukh. *Experimental Investigation of Flanged Tube Retrofitting Effects on Reinforced Concrete Beams with Web Openings*. 2025.

[2] M. K. Ghali, M. Said, T. Mustafa, and A. A. El-Sayed, *Behaviour of T-shaped* RC *deep beams with openings under different loading conditions*, Structures, 2021, vol. 31: Elsevier, pp. 1106-1129.

[3] M. R. Khalaf and A. H. A. Al-Ahmed, *Shear strength of reinforced concrete deep beams with large openings strengthened by external prestressed strands*, *Structures*, 2020, vol. 28: Elsevier, pp. 1060-1076.

[4] X. Nie, S. Zhang, and T. Yu, *Behavior of RC beams with a fiber-reinforced polymer (FRP)-strengthened web opening*, *Composite* Structures, 2020, vol. 252, p. 112684.

[5] A. Arabzadeh and H. Karimizadeh, *Experimental study of RC deep beams with opening and FRP composites installed by* means *of EBR and EBROG methods*, *Construction and Building Materials, 2019,* vol. 208, pp. 780-791.

[6] C. Aksoylu, Ş. Yazman, Y. O. Özkılıç, L. Gemi, and M. H. Arslan, Experimental *analysis of reinforced concrete shear deficient beams with circular web openings*

strengthened by CFRP composite, *Composite Structures,* 2020, vol. 249, p. 112561.

[7] A. Amer, *Strengthening of beam openings in flexural region for* different *shapes*, *Civil* Engineering Research Magazine*,* 2013*,* vol. 35(1).

[8] M. El-Samny, H. Ezz-ELdeen, and M. Elsepahy, *Experimental and Analytical Study of Strengthening Reinforced Concrete Beams with Openings*, *International Journal of Applied* Engineering Research, 2018*,* vol. 13(7), pp. 4934-4950.

[9] Olanitori, L. M., Otuaga, M. P., & Oso, I. A. *Effect of Large Openings on Bending Strength of Reinforced Concrete Beam*. Journal of Engineering Research and Reports. 2022, Vol. 23(8), pp. 1-10.

[10] M. Mansur and K.-H. Tan, *Concrete beams with openings: analysis and design*. New York: CRC Press, 1999. ISBN 0-8493-7435-9.

[11] J. Nie, C. Cai, H. Wu, and J. Fan, *Experimental and theoretical study of steel–concrete composite beams with openings in concrete flange*, Engineering structures*,* 2006, 28(7), pp. 992-1000.

[12] Mansur, M. A., Lee, Y. F., Tan, K. H., & Lee, S. L. *Tests on RC* continuous *beams with openings*. Journal of Structural Engineering, 1991, 117(6), p1593-1606.

[13] T. El-Maaddawy and B. El-Ariss, "*Behavior of* concrete *beams with short shear span and web opening strengthened in shear with CFRP composites*," Journal of Composites for Construction, 2012*,* vol. 16, no. 1, pp. 47-59.

[14] N. Somes and W. Corley, *Circular openings in webs of continuous* beams, Special Publication*,* 1974, vol. 42, pp. 359-398.

[15] J. Lee, C. Li, and Y. Lee, *Experimental study on shear strength of reinforced* concrete *continuous deep beams with web opening*, in the 14th World Conference on Earthquake Engineering, 2008, pp. 12-17.

[16] M. A. Mansur, *Effect of openings on the behavior and strength of R/C beams in shear*, Cement and concrete composites*,* 1998, 20(6), pp. 477-486.

[17] Mondal, S., Bandyopadhyay, J., & Tan, C. P. *Reinforced concrete beams with web openings: A state-of-the-art review*. International Journal of Civil and Structural Engineering, 2011, 1(4), 787–797.

[18] Mondal, Subhajit, J. N. Bandyapadhya, and Chandra Pal Gautam. *Strengthening and rehabilitation of reinforced concrete beams with an opening*. International Journal of Civil & Structural Engineering 2.1 2011: 127-137.

[19] Hassan BR, Abdul-Kadir MR, Ghafoor KK. *Strengthening of reinforced concrete T-beam with web opening*. Sulaimani Journal for Engineering Sciences. 2017, 14(5):156-72.

[20] Meleka, Nageh Nassif. *Flexural and Shear Strengthening of* RC *Beams with Large Openings by Steel or CFRP Plates*. ERJ. Engineering Research Journal 43.4 2020: 327-336.

[21] Mondal, S. (2011). *Strengthening and rehabilitation of reinforced concrete beams with an opening*, Int. J. of Civil and Structural Engineering, 2011, 2(1), pp. 127–138.

[22] Akhila, P.S., Arathi, S., *Analysis of Beam Openings Strengthened* by Carbon *Fibre Reinforced Polymer (CFRP) Using ANSYS*, Int. J. Sci. Res., 2016, 5(7), pp. 1097–1101.

[23] Chin, S.C., Shafiq, N., Nuruddin, M.F. (2016). Behavior of RC beams with CFRP-strengthened openings, Struct. Concr., 2016, 17(1), pp. 32–43.

[24] Miruthun, G., et al. *Experimental investigation on strengthening of reinforced concrete beams using GFRP laminates*. Materials Today: Proceedings 37 2021: 2744-2748.

[25] Amer, A., *Strengthening of beam openings in the* flexural *region for different shapes*, Civ. Eng. Res. Mag., 2013, 35(1).

[26] Akhila, P.S., Arathi, S. *Analysis of Beam Openings Strengthened* by *Carbon Fibre Reinforced Polymer (CFRP) Using ANSYS*, Int. J. Sci. Res., 2016, 5(7), pp. 1097–1101.

[27] Chin, S.C., Shafiq, N., Nuruddin, M.F. *Behaviour of RC beams with CFRP-strengthened openings*, Struct. Concr., 2016, 17(1), pp. 32–43.

[28] Abdullah, W., Omar, A., & Rafiq, S.K., Experimental *Work on Using* Fully *Wrapped Post-Tensioned Metal Straps Around Normal Reinforced Concrete Beams to Increase Flexural Strength of RC Beams*. *Suleimani J. Eng. Sci*, 2021, *8*.

[29] Frangou, M., K. Pilakoutas, and S. Dritsos. *Structural repair/strengthening of RC* columns. Construction and building materials, 1995, 9(5): 259-266.

[30] Y. Yang, S. Feng, Y. Xue, Y. Yu, H. Wang, and Y. Chen, *Experimental study on shear behavior of fire-damaged reinforced concrete T-beams retrofitted with prestressed steel straps*, Constr. Build. Mater., 2019, vol. 209, pp. 644–654.

[31] F. Amsyar, M. C. Khun, W. Omar, A. Zawawi Awang, and S. Poi Ngian, *Behaviour* of *lightweight foamed concrete with pretensioned Ing steel straps confinement*, IOP Conf. Ser. Earth Environ. Sci., 2019, 220(1).

[32] Y. Helal, R. Garcia, K. Pilakoutas, M. Guadagnini, and I. Haji Rasouliha, *Strengthening of short splices in RC beams using Post-Tensioned Metal Straps*,

Mater. Struct. Constr., 2016, vol. 49(1–2), pp. 133–147.

[33] C. K. Ma, A. Z. Awang, W. Omar, M. Liang, S. W. Jaw, and M. Azimi, Flexural *capacity* enhancement *of rectangular high-strength concrete columns confined with posttensioned steel straps: experimental investigation and analytical modelling,* Struct. Concrete, 2016, vol. 17(4), pp. 668–676.

[34] C. K. Ma, A. Z. Awang, and W. Omar, *Slenderness effect and upper-bound slenderness limit of SSTT-confined HSC column*, Int. J. Struct. Eng., 2014, vol. 5(3), pp. 279–286.

[35] C. K. Ma, R. Garcia, S. C. S. Yung, A. Z. Awang, W. Omar, and K. Pilakoutas, strengthening *of pre-damaged concrete cylinders using post-tensioned steel straps*, Proc. Inst. Civ. Eng. Struct. Build., 2019, 172(10), pp. 703–711.

[36] C. K. Ma, A. Z. Awang, W. Omar, and L. Maybelle, *Experimental* tests *on SSTT confined HSC columns*, Mag. Concrete. Res., 2014, vol. 66(21).

[37] Moghaddam, H., M. Samadi, and S. Mohebbi. *RC members strengthening by lateral post-tensioning of external metal strips*. In Int. Earthquake. Symp. KOCAEU, 2007, vol. 1995, pp. 454-62.

[38] Garcia, R., et al. *Seismic strengthening of deficient RC buildings using post-tensioned metal straps: an experimental investigation*. Proceedings of the 15WCEE, Lisbon, Portugal, 2012: 24-28.

[39] Moghaddam, Hasan, et al., *Axial compressive behavior of concrete* actively *confined by metal strips; part A: experimental study*. Materials and Structures construction, 2010, 43(10): 1369-1381.

[40] H. Moghaddam, M. Samadi, and K. Pilakoutas, *Compressive* behavior *of concrete actively confined by metal strips, part B: Analysis*, Materials and Structures Construction, 2010, vol. 43(10), pp. 1383–1396.

[41] Helal, Y., García, R., Pilakoutas, K., Guadagnini, M., & Hajirasouliha, I. *Strengthening of short splices in RC beams using Post-Tensioned Metal Straps. Materials and Structures*, 2016, 49(1), 133-147.

[42] Abdullah, W., & Rafiq, S. K. *Flexural strengthening of beams using post-tensioned metal straps fully wrapped around steel channels anchored to normal steel reinforced concrete beams*. Plos one, 2021, 16(6), e0253816.

[43] ACI 211.1-91, *Standard Practice for Selecting Proportions for Normal, Heavyweight, and Mass Concrete*, American Concrete Institute, 1991.

[44] ASTM C33-18, "*Standard specification for concrete* aggregates." ASTM International. www.astm.org, 2018.

[45] American Concrete Institute, ACI 318-25," *Building Code Requirements for Structural Concrete and* Commentary*, American Concrete Institute*", 2019.

دراسة تجريبية حول تقوية انحناء عوارض الخرسانة المسلحة ذات الفتحات باستخدام أحزمة معدنية عالية التحمل

المستخلص

ثبت علمياً أن فتحات في العوارض الخرسانية تؤدي الى تقليل مقاومتها ألإنشائية، مما يجعل التدعيم أمراً ضرورياً لتحسين سعة التحمل، و نمط ألإنهيار، و الممطولية، و حمل التشقق ألأول. و هنالك إمكانية تدعيم العوارض الخرسانية المسلحة ذات الفتحات بإستخدام قضبان التسليح الداخلية او البوليمرات المسلحة بالألياف(FRP)، إلا إن الدراسات السابقة لم تتطرق إلى إستخدام ألأحزمة المعدنية كأداة للتدعيم. لذلك تبحث هذه الدراسة في تأثير استخدام أحزمة معدنية عالية التحمل (HDMS) لتقوية عوارض الخرسانة المسلحة ذات الفتحات. شمل البرنامج التجريبي اختبار سبع عوارض خرسانية مسلحة بأبعاد عمق ٢٥٠ ملم وعرض ١٥٠ ملم وطول صافي يبلغ ١٢٠٠ ملم. احتوت ست منها على فتحة في منتصف امتداد العوارض الخرسانية المسلحة، بينما كانت إحداها عينة تحكم صلبة وغير حاوية على الفتحة. تمثلت المتغيرات الرئيسية في شكل الفتحة (دائرية و مربعة) و طريقة تطبيق احزمة (HDMS) (رأسياً و افقياً). صممت الفتحة الدائرية بقطر ١١٠ملم و المربعة بأبعاد لضمان تساوي مساحات المقطع تقريباً. أظهرت النتائج ان التدعيم ألأفقي بإستخدام أحزمة HDMS أدى إلى زيادة سعة تحمل ألأحمال بنسبة ١٠% للفتحات الدائرية و ١٦% للفتحات المربعة مقارنة بالعينة الصلدة التحكمية. أما فيما يخص التدعيم الرأسي في تحسين حمل التشقق ألأول، فقد ازدادت بنسبة ١٦% للفتحات الدائرية و ٥% للفتحات المربعة، و ذلك مقارنة بالعوارض غير المدعمة التي تحتوي على فتحات.

الكلمات المفتاحية:

العوارض، اشكال الفتحات، طرق التقوية، مواد التقوية.

Figure 1: Opening at the flexure region.[1].

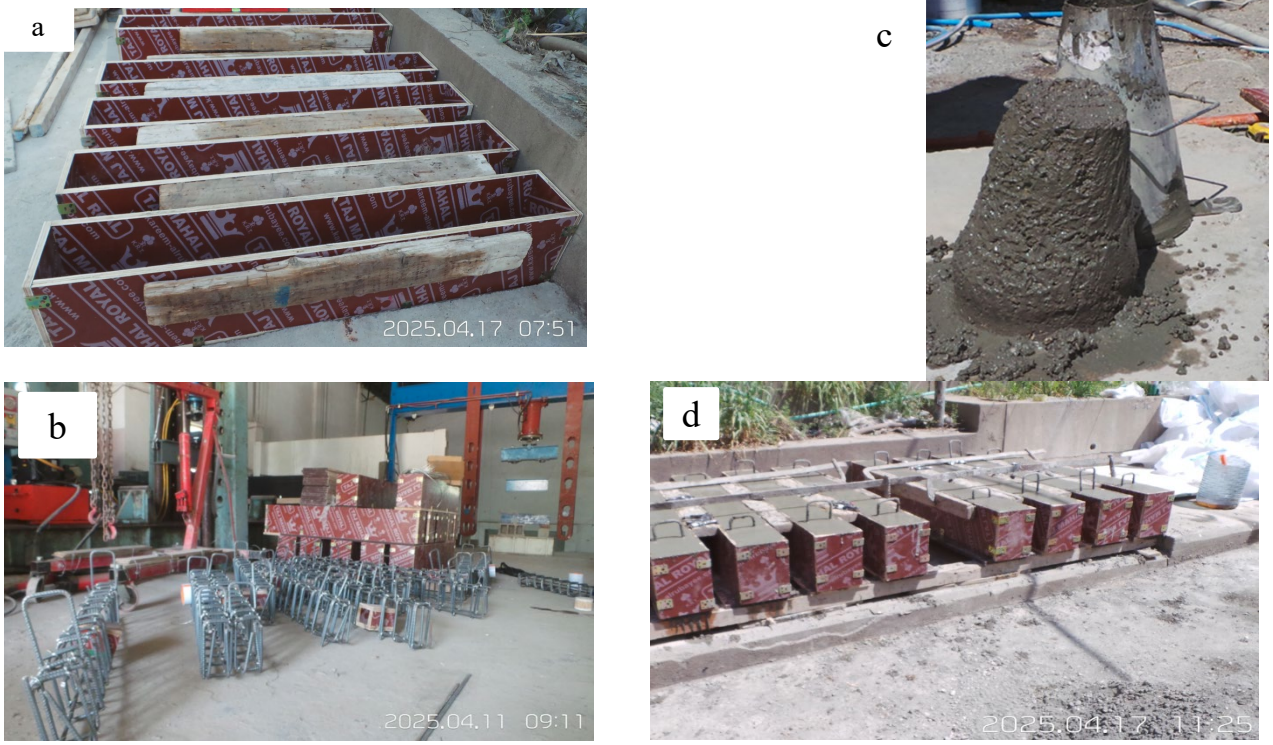

Figure 2: Illustration of the specimen preparation process, including (a) formwork process, (b) reinforcement tightening, (c) slump test, and (d) concrete Casting.

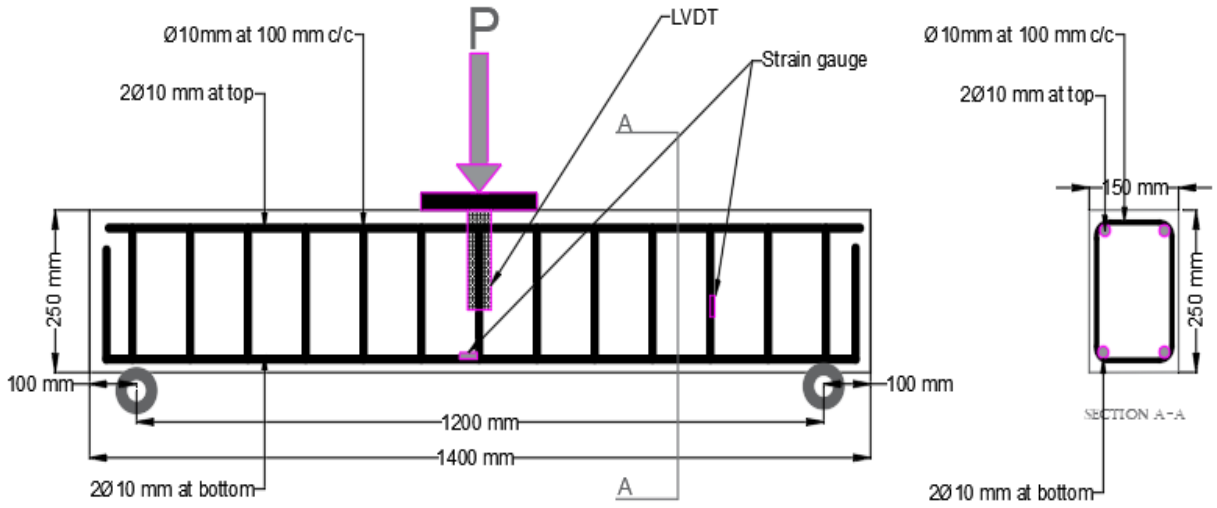

Figure 3: Control beam layout and point load location.

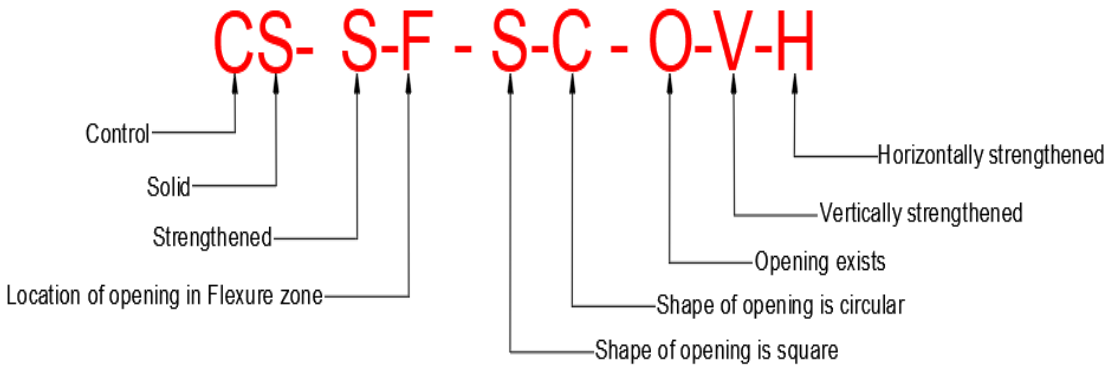

Figure 4: Beam symbols summary.

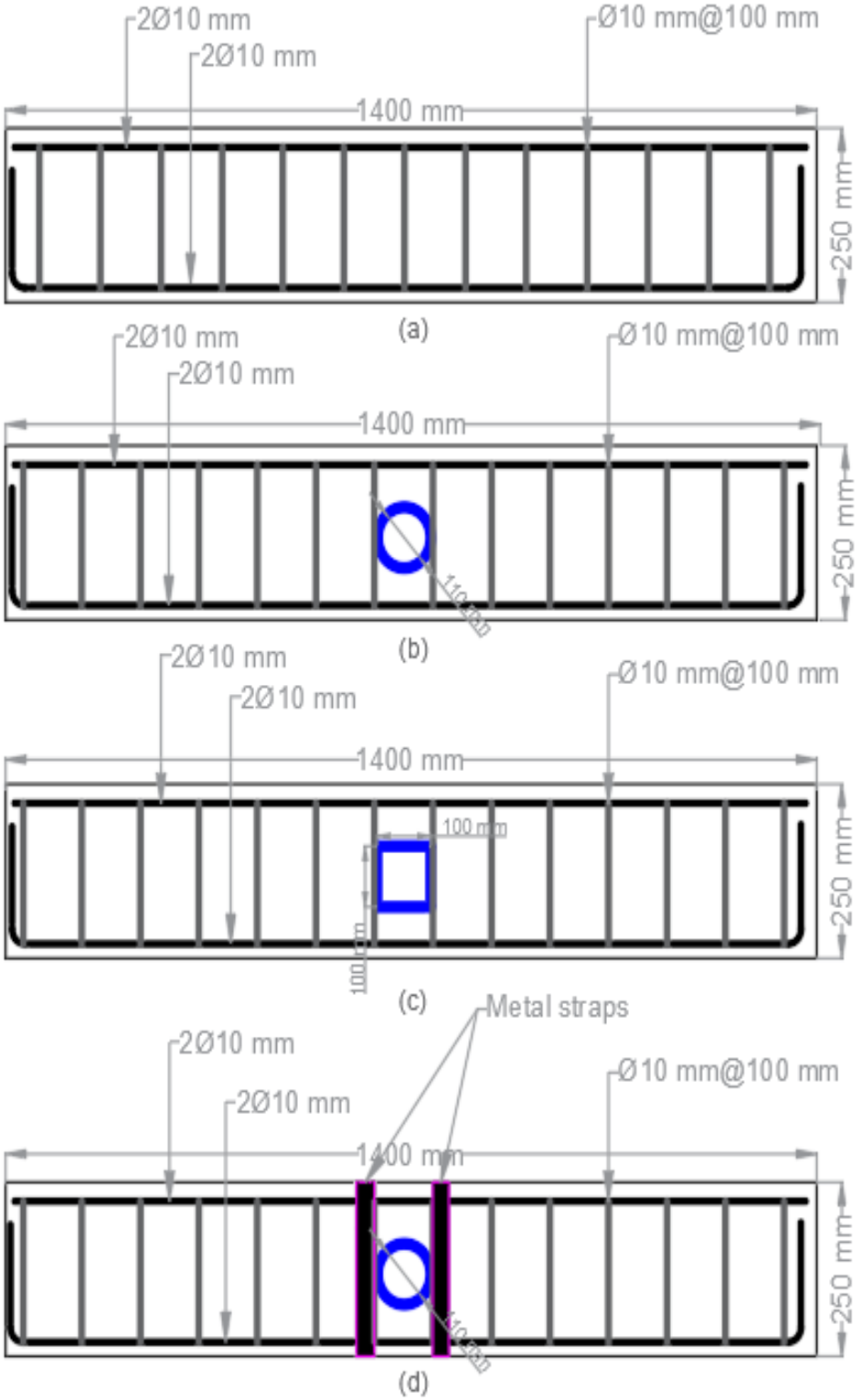
2Ø10 mm
2Ø10 mm
Ø10 mm@100 mm
1400 mm
250 mm
(a)
2Ø10 mm
2Ø10 mm
Ø10 mm@100 mm
1400 mm
250 mm
(b)
2Ø10 mm
2Ø10 mm
Ø10 mm@100 mm
1400 mm
100 mm
250 mm
(c)
Metal straps
2Ø10 mm
2Ø10 mm
Ø10 mm@100 mm
1400 mm
250 mm
(d)

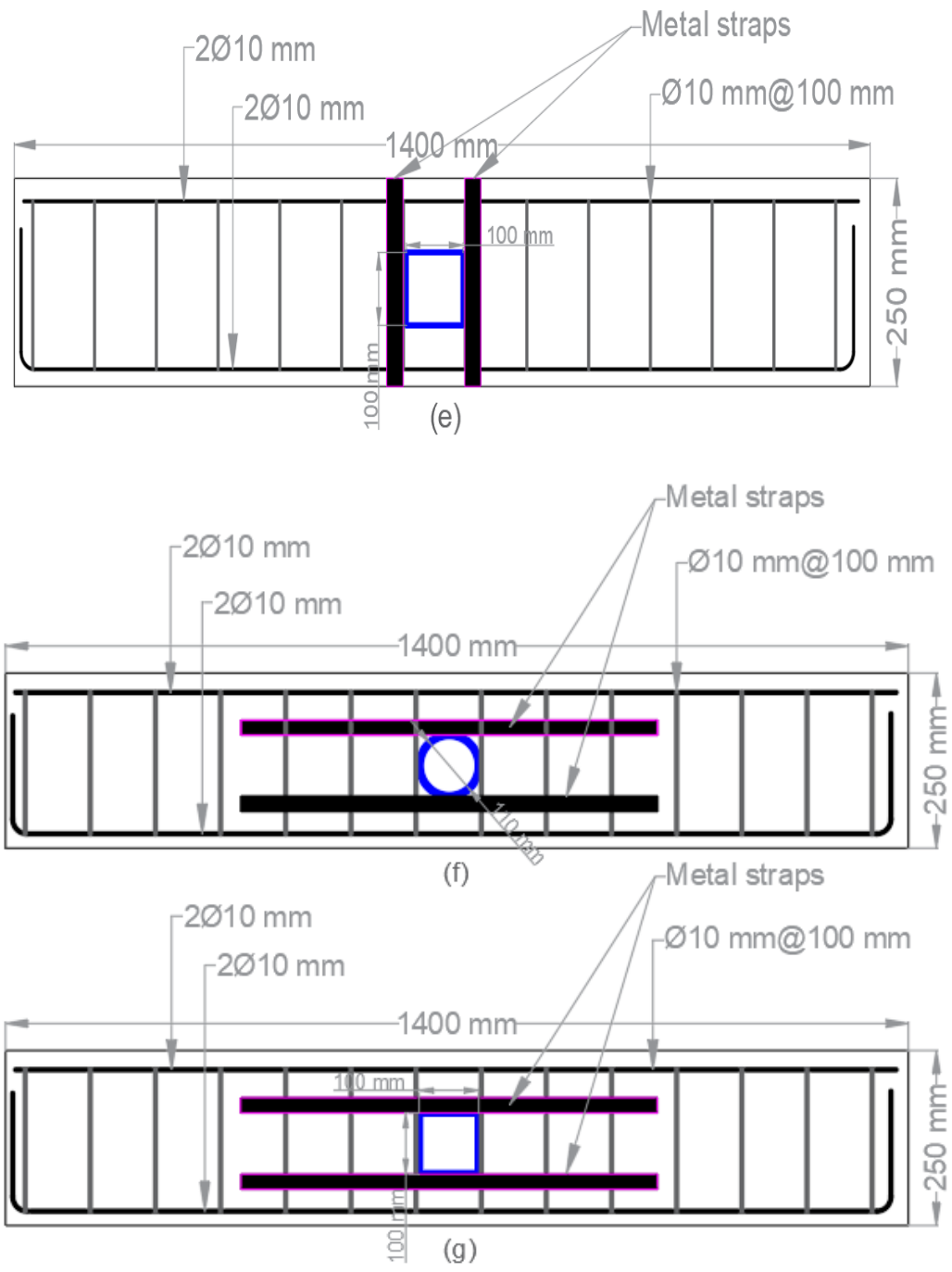

Figure 5: Layout of the tested beams (a) CS, (b) CFCO, (c) CFSO, (d) SFCOV, (e) SFSOV, (f) SFCOH and (g) SFSOH.

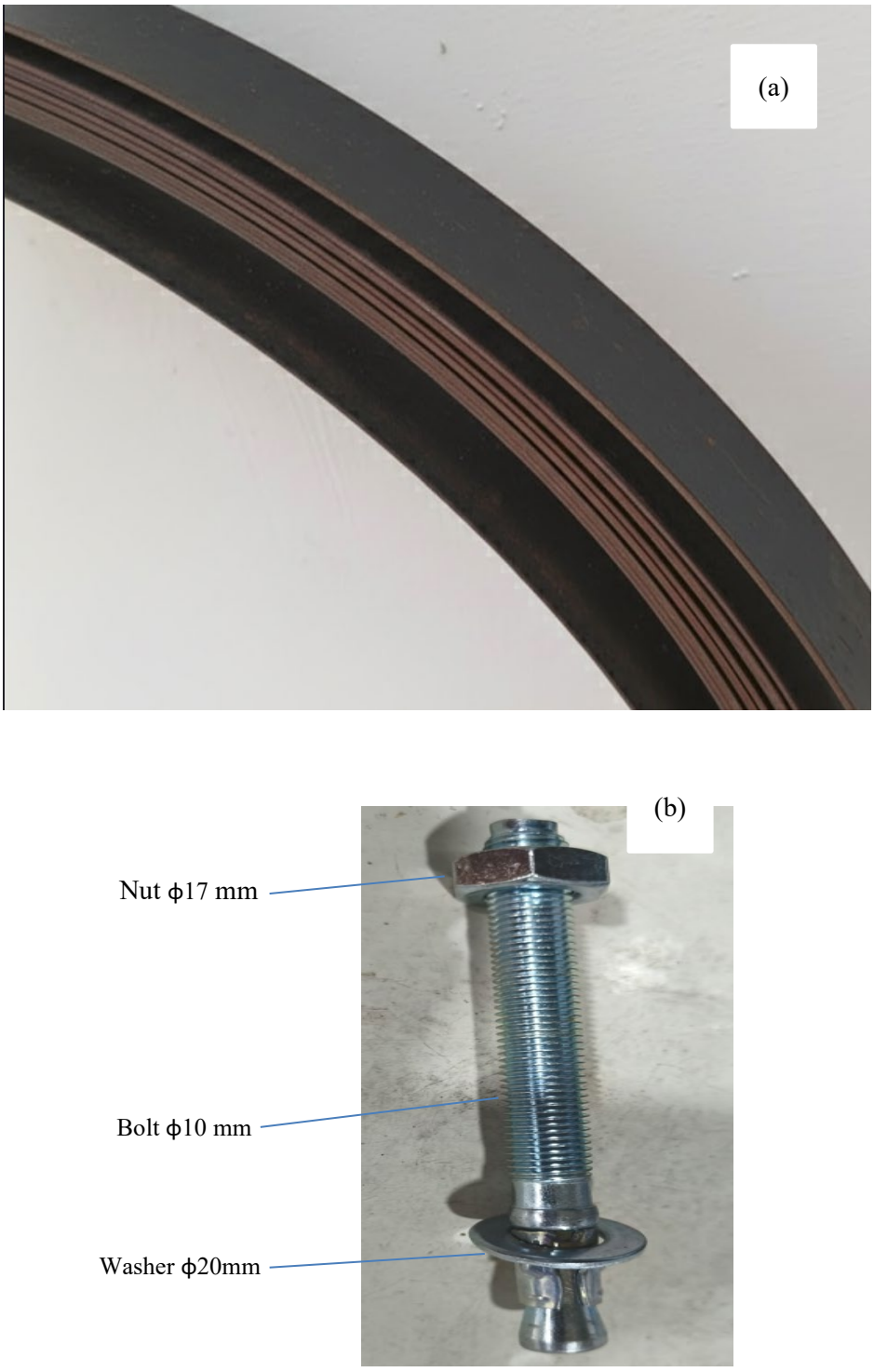

Figure 6: Materials for strengthening (a) Metal strap, (b) Bolt with nut and washer

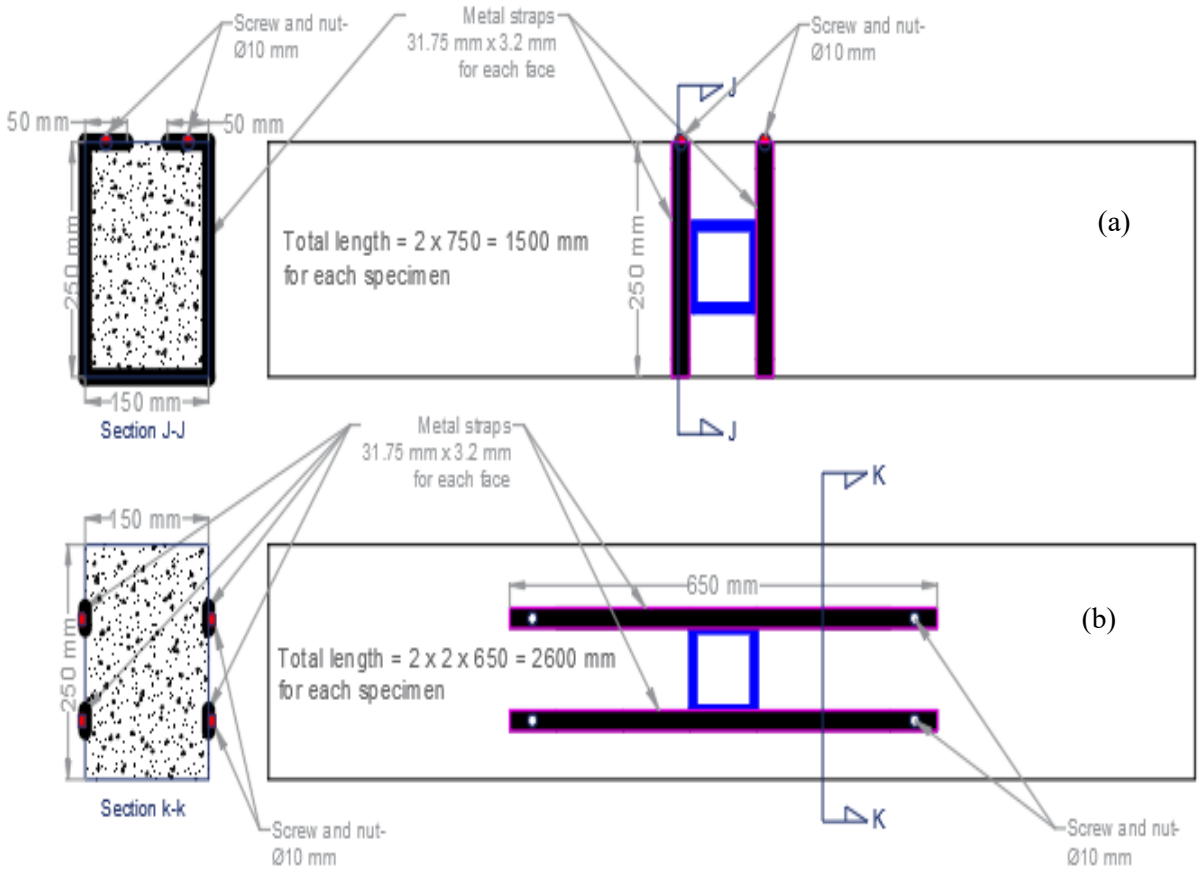

Figure 7: Strengthened beams with HDMS (a) Beam strengthening vertically (b) Beam strengthening horizontally

Table 1: Compressive strength of the cylinders

Cylinder label	Average Length (mm)	Average Diameter (mm)	Load (kN)	Compressive strength f'_c (MPa)
Cylinder 1	300	150	440.33	24.93
Cylinder 2	300	150	524.05	29.67
Cylinder 3	300	150	482.89	27.34
Average value of compressive strength f'_c				27.31

Table 2: The results of the beam specimens

No.	Specimen name	P_{cr} (kN)	P_y (kN)	P_u (kN)	P_u / P_{solid}	P_u / $P_{control}$	Δy (mm)	Δu (mm)	Δu / Δy	Mode of Failure	Crack width (mm)
1	CS	21	47.9	73.5	100%	100%	1.71	16.8	9.82	Flexure	11.0
2	CFCO	22.2	53.5	72.2	98.23%	100%	1.35	7.2	5.33	Flexure	5.0
3	CFSO	23.4	54.9	72.8	99.05%	100%	2.36	17.9	7.58	Flexure	6.0
4	SFCOV	25.8	53.8	75.7	102.99%	104.85%	1.27	9.0	7.09	Flexure	8.0
5	SFSOV	24.6	55.1	76.9	104.63%	105.63%	3.12	31.6	10.13	Flexure	10.0
6	SFCOH	18.0	51.0	80.9	110.07%	112.05%	2.95	11.7	3.97	Flexure	11.0
7	SFSOH	15.0	52.1	85.0	115.67%	116.72%	2.0	27.7	13.85	Flexure	9.0

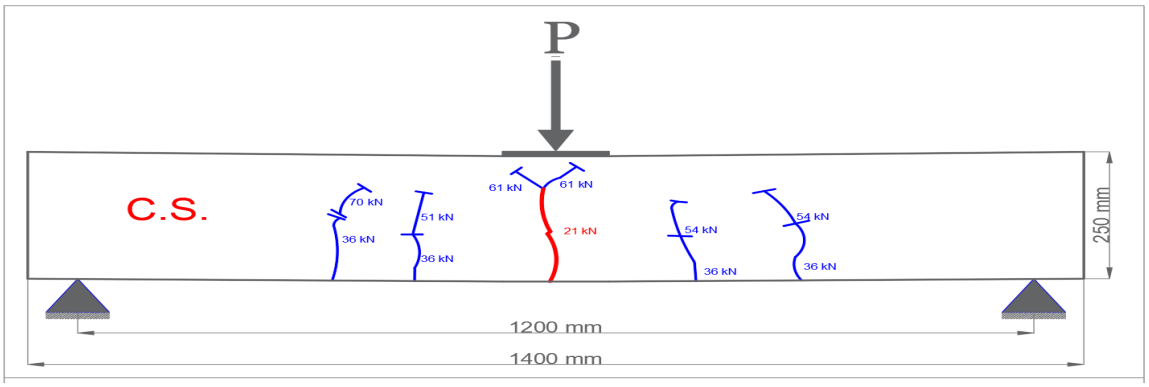
P
C.S.
70 kN
36 kN
51 kN
36 kN
61 kN
61 kN
21 kN
54 kN
36 kN
54 kN
36 kN
250 mm
1200 mm
1400 mm

(a)

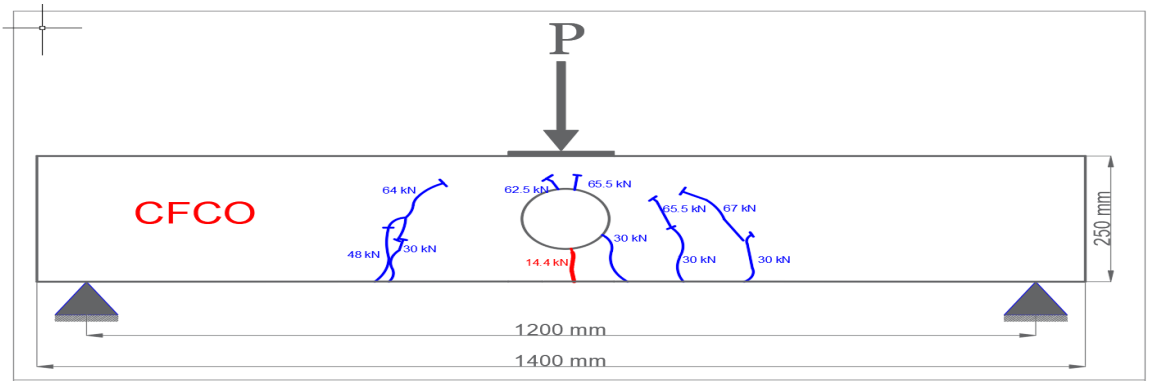
P
CFCO
64 kN
48 kN
30 kN
62.5 kN
65.5 kN
30 kN
14.4 kN
65.5 kN
67 kN
30 kN
30 kN
250 mm
1200 mm
1400 mm

(b)

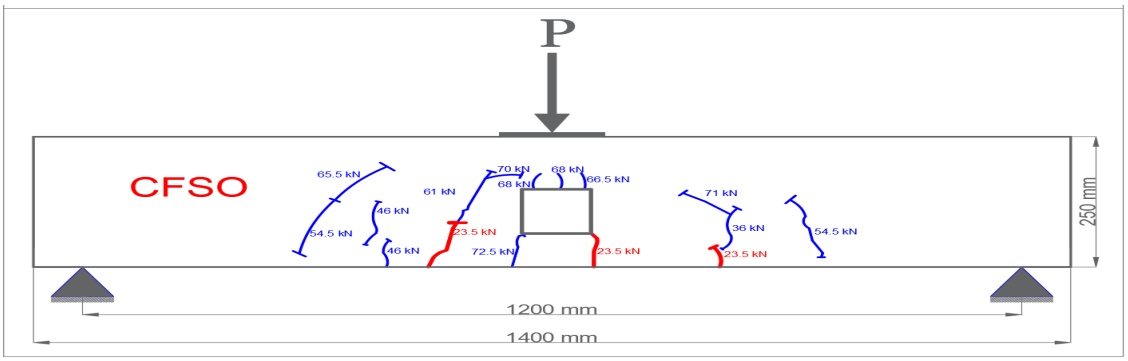
P
CFSO
65.5 kN
54.5 kN
46 kN
46 kN
61 kN
70 kN
68 kN
68 kN
86.5 kN
23.5 kN
72.5 kN
23.5 kN
71 kN
36 kN
23.5 kN
54.5 kN
250 mm
1200 mm
1400 mm

(c)

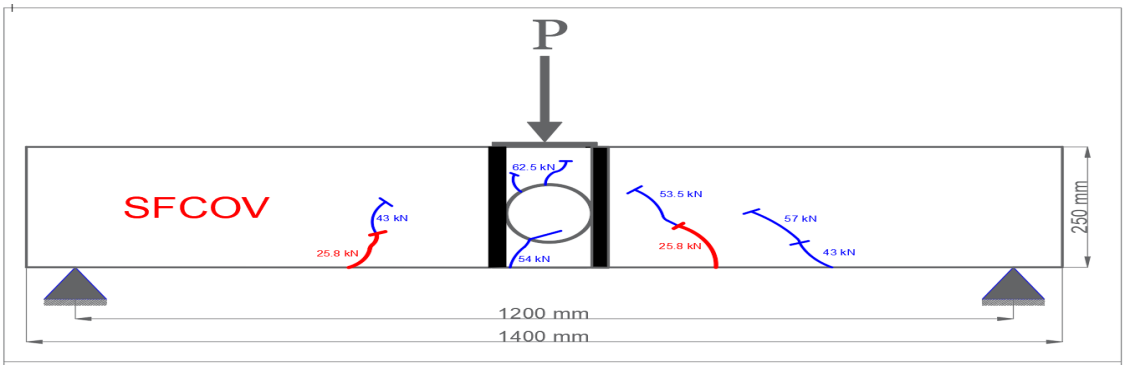
P
SFCOV
43 kN
25.8 kN
62.5 kN
54 kN
53.5 kN
25.8 kN
57 kN
43 kN
250 mm
1200 mm
1400 mm

(d)

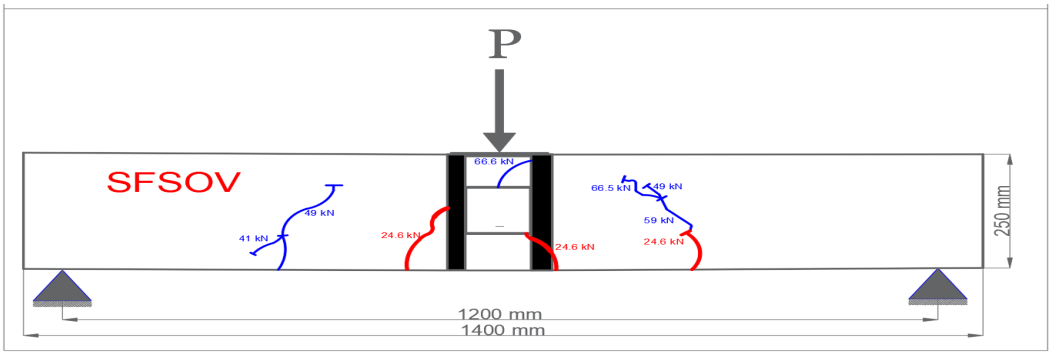

(e)

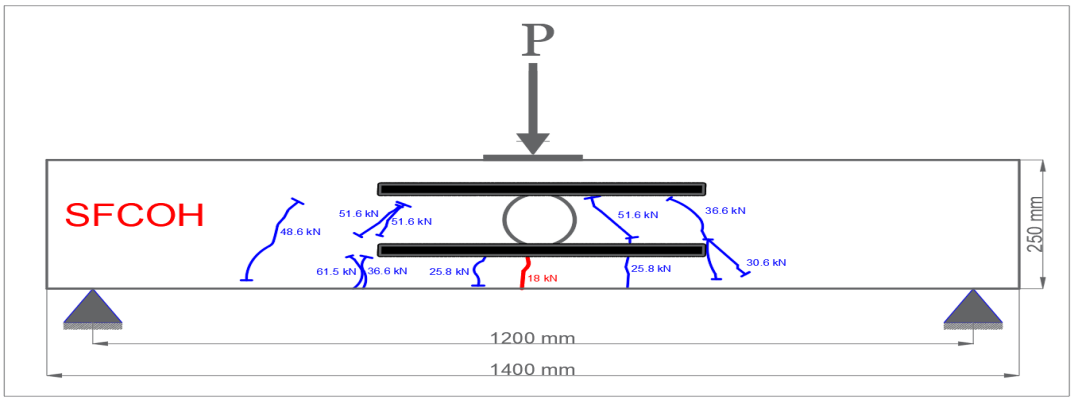

(f)

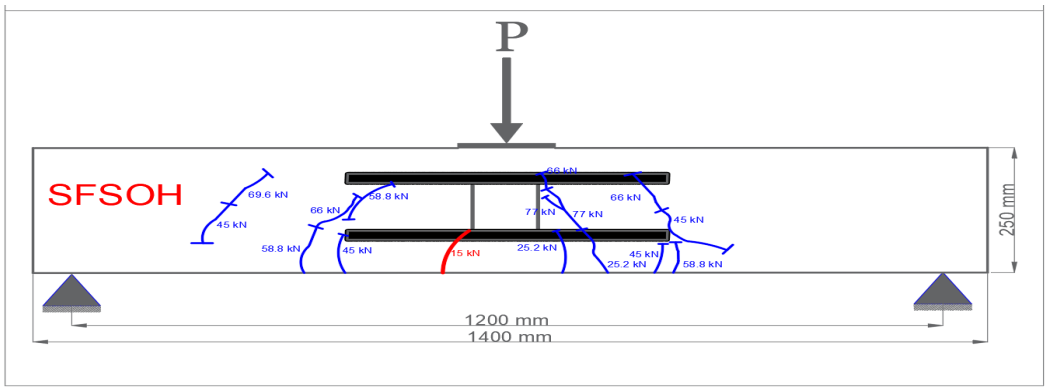

(g)

Figure 8: Crack Patterns: (a) CS, (b) CFCO, (c) CFSO, (d) SFCOV, (e) SFSOV, (f) SFCOH, and (g) SFSOH.

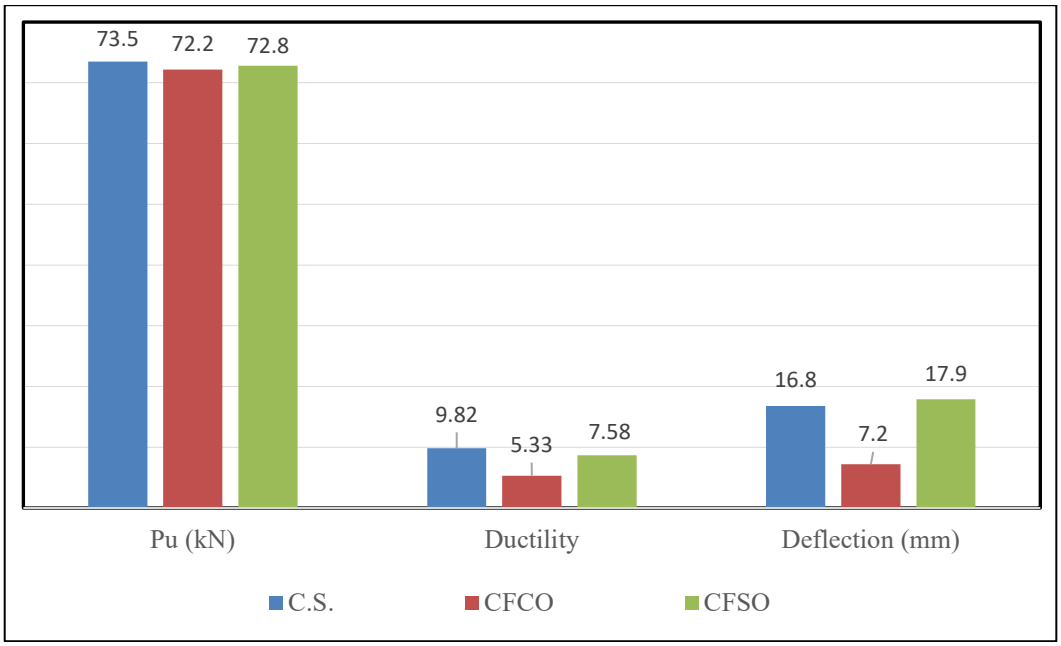

Figure 9: Ultimate load, Ductility, and Deflection of CS, CFCO, and CFSO.

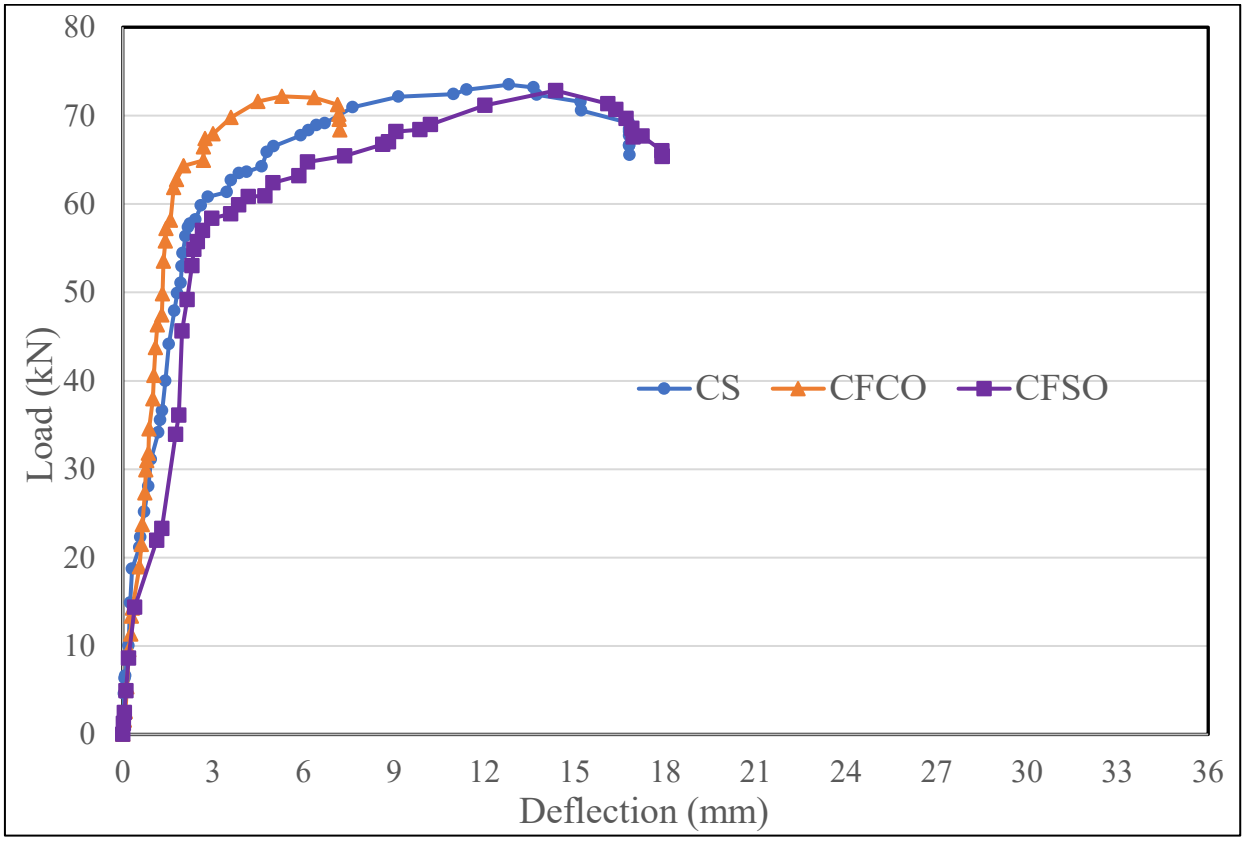

Figure 10: Load deflection diagram between CS, CFCO, and CFSO.

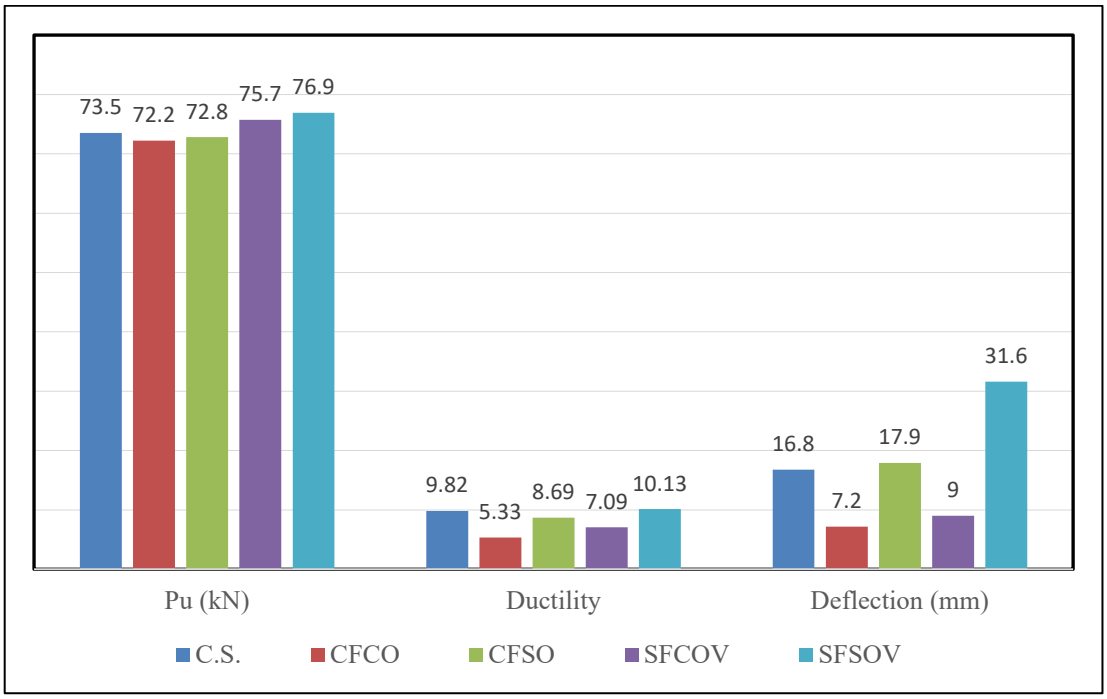

Figure 11: Ultimate load, Ductility, and Deflection of CS, CFCO, CFSO, SFCOV, and SFSOV

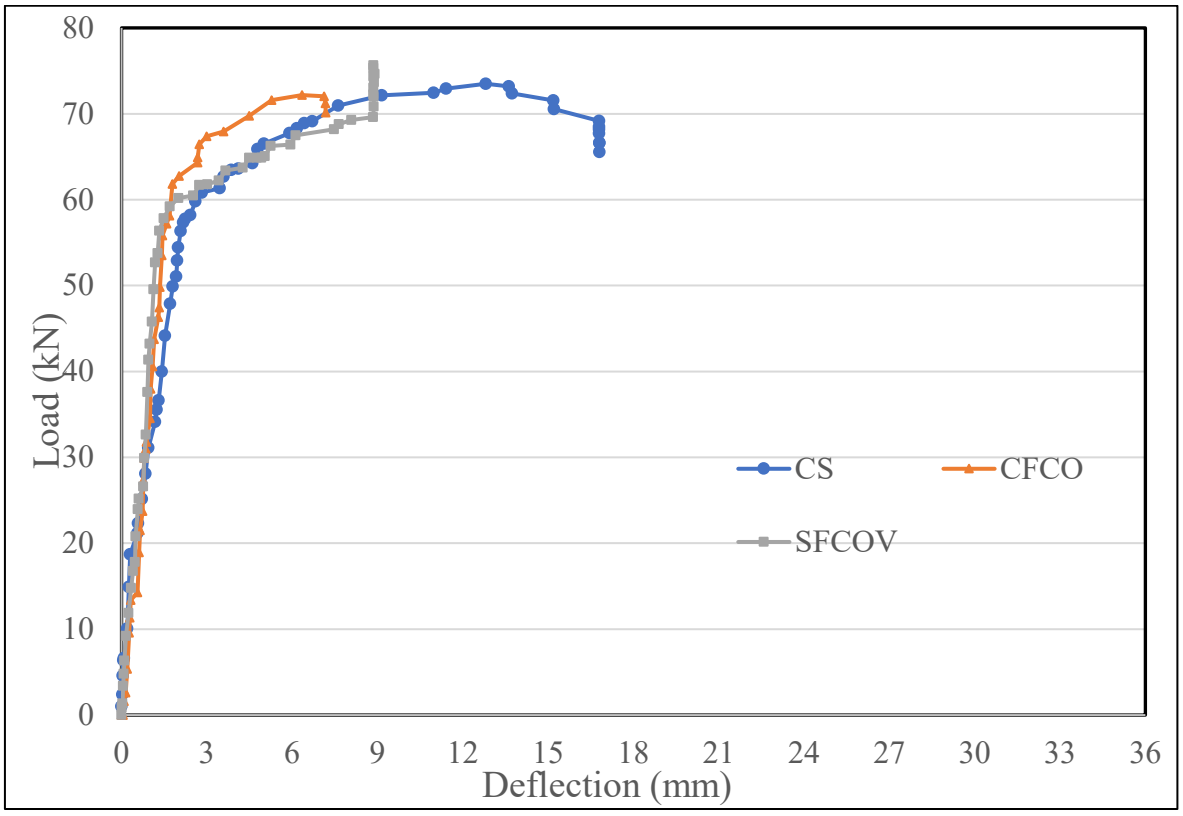

Figure 12: Load-deflection diagram between CS, CFCO, and SFCOV.

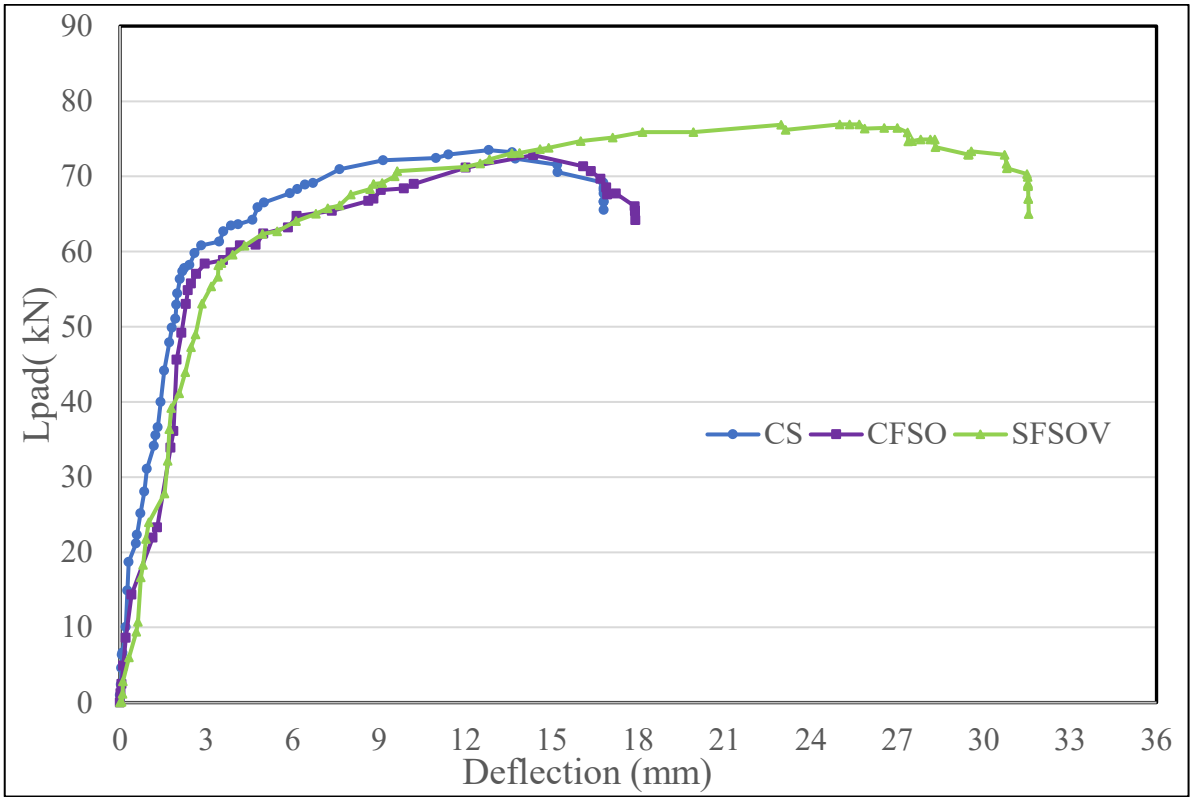

Figure 13: Load-deflection diagram between CS, CFSO, and SFSOV

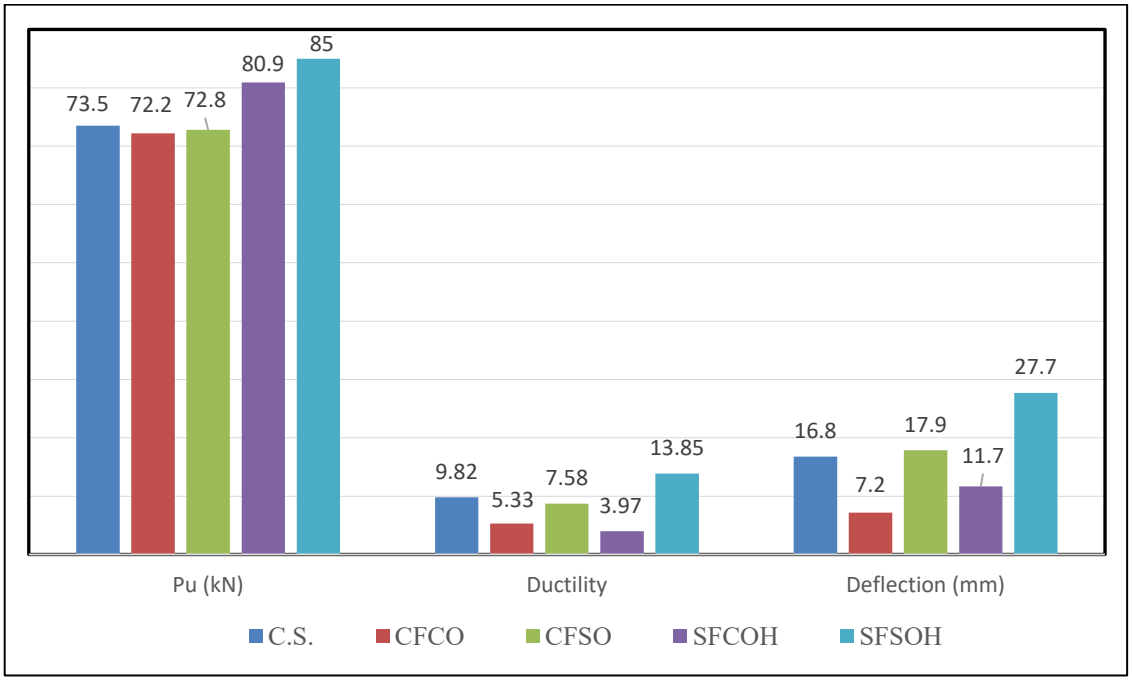

Figure 14: Ultimate load, Ductility, and Deflection of CS, CFCO, CFSO, SFCOH, and SFSOH.

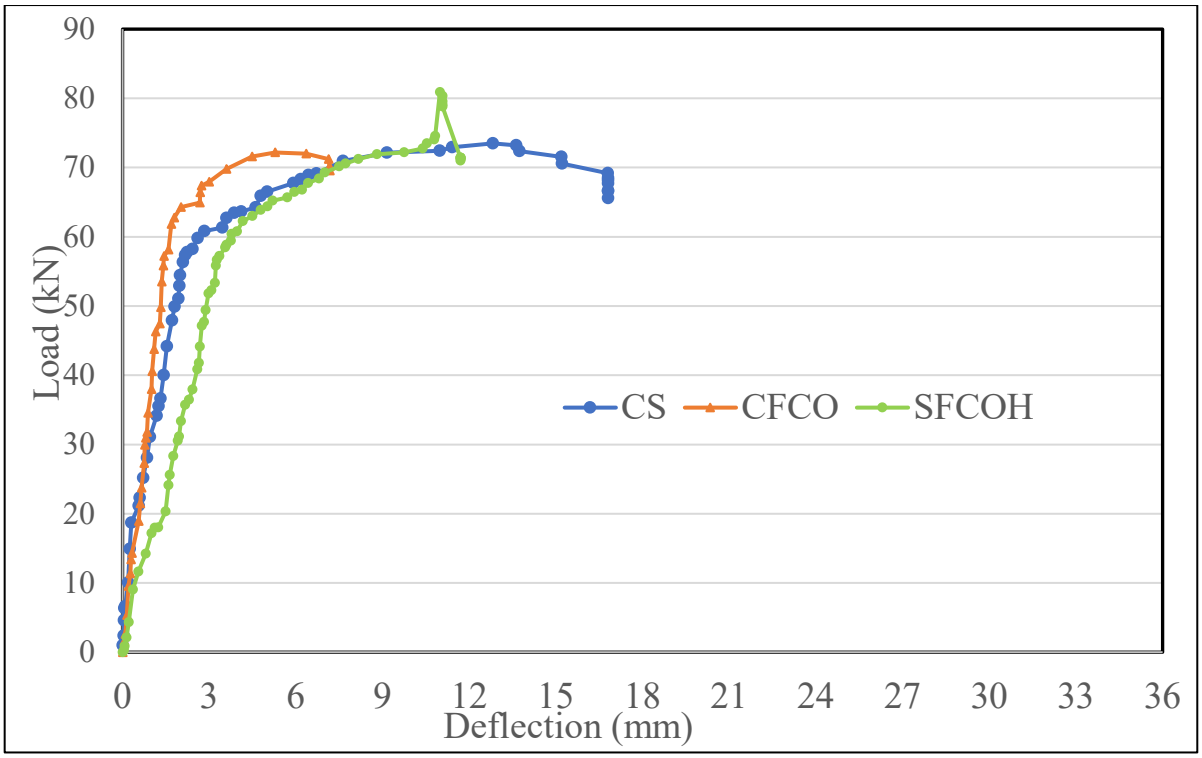

Figure 15: Load-deflection diagram between CS, CFCO, and SFCOH.

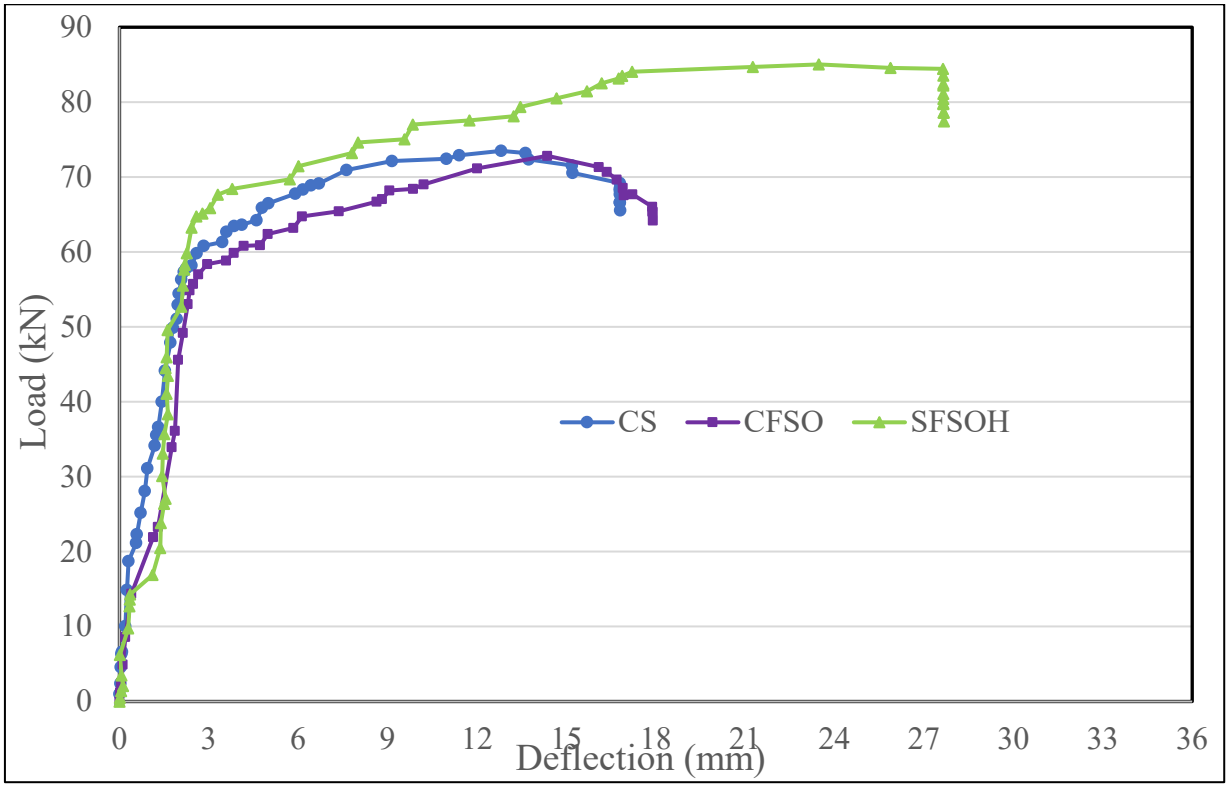

Figure 16: Load-deflection diagram between CS, CFSO, and SFSOH.

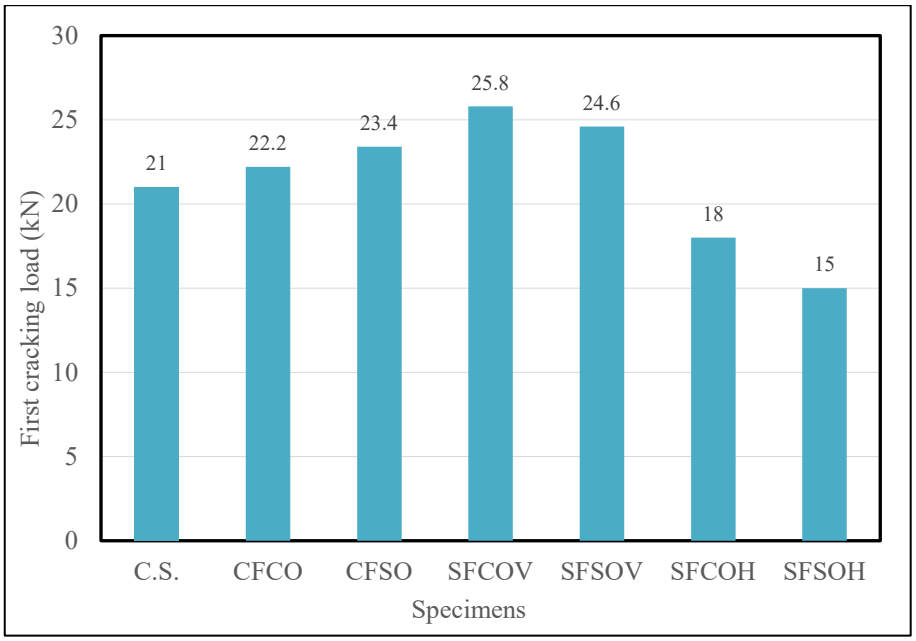

Figure 17: First cracking load of CS, CFCO, CFSO, SFCOV, SFSOV, SFCOH, and SFSOH.

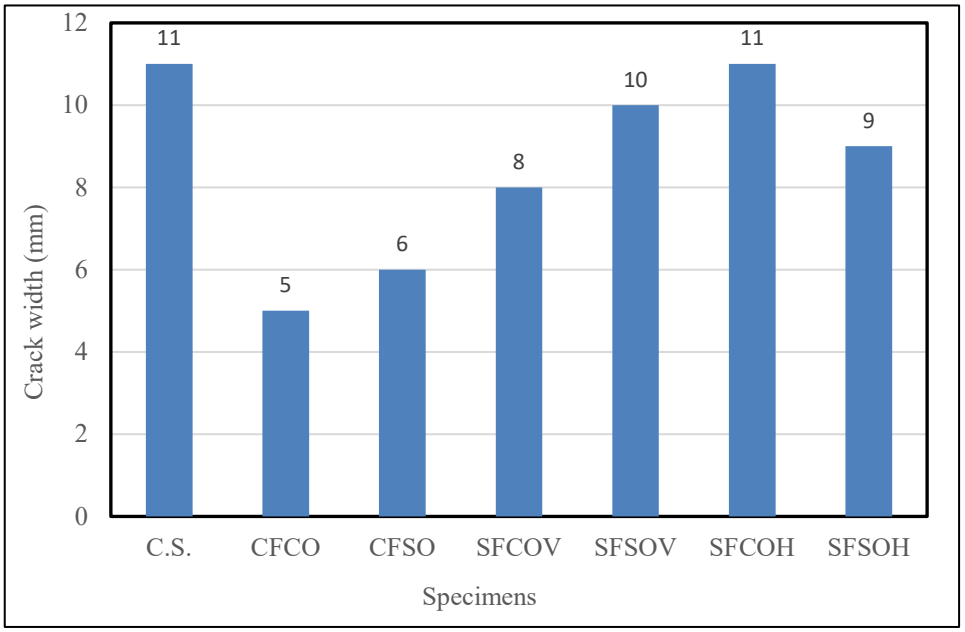

Figure 18: Crack width of CS, CFCO, CFSO, SFCOV, SFSOV, SFCOH, and SFSOH.

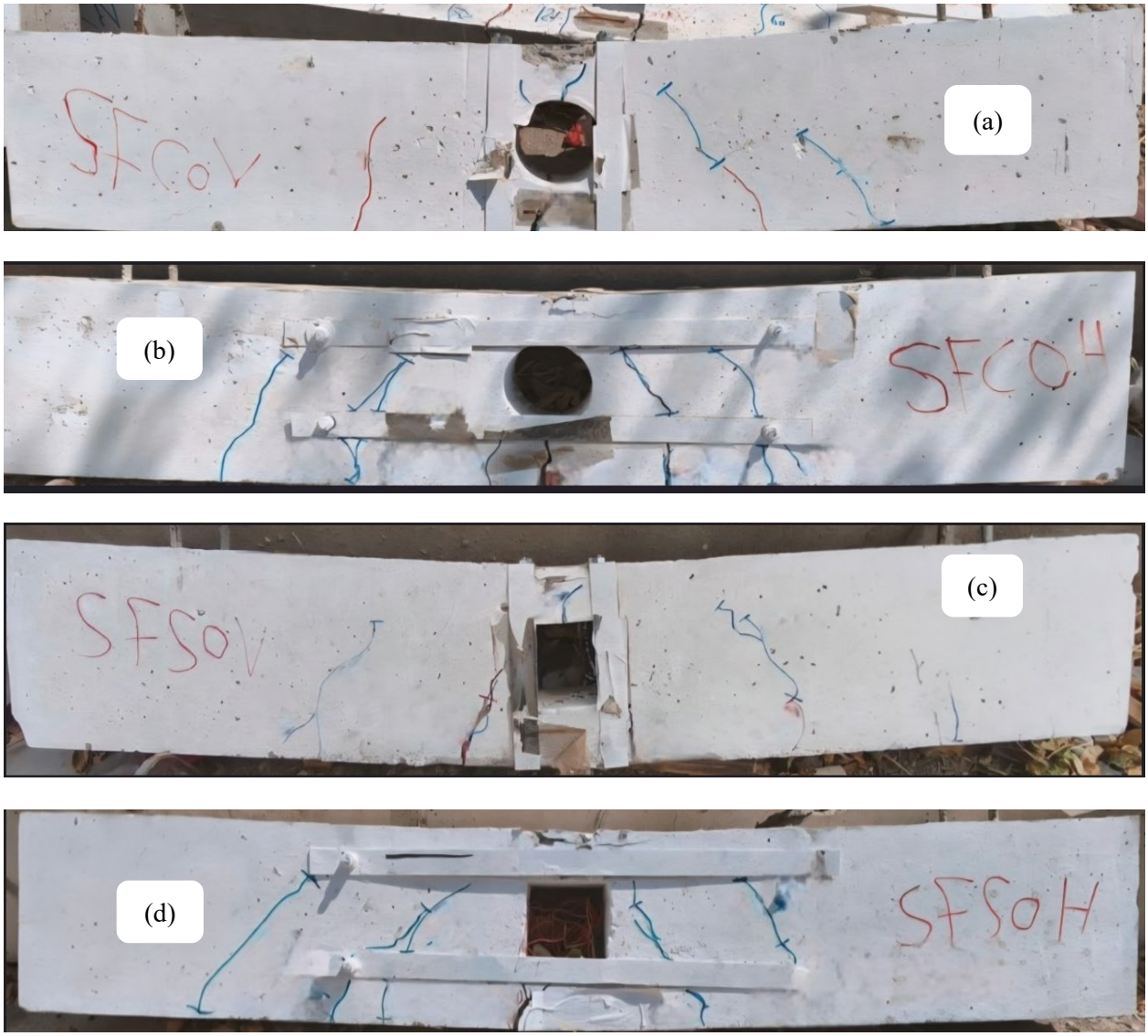

Figure 19: The tested specimens (a)SFCOV, (b)SFCOH, (c)SFSOV, and (d) SFSOH

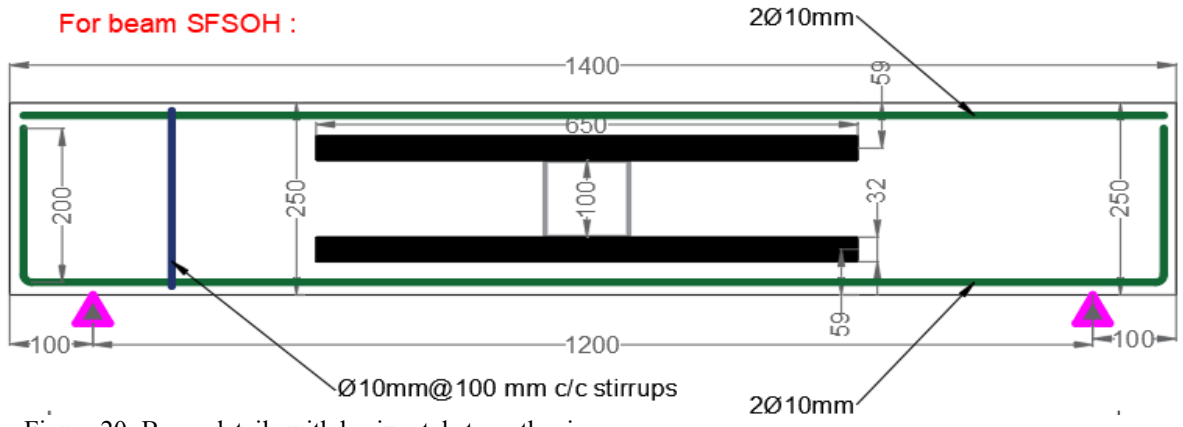

Figure 20: Beam details with horizontal strengthening

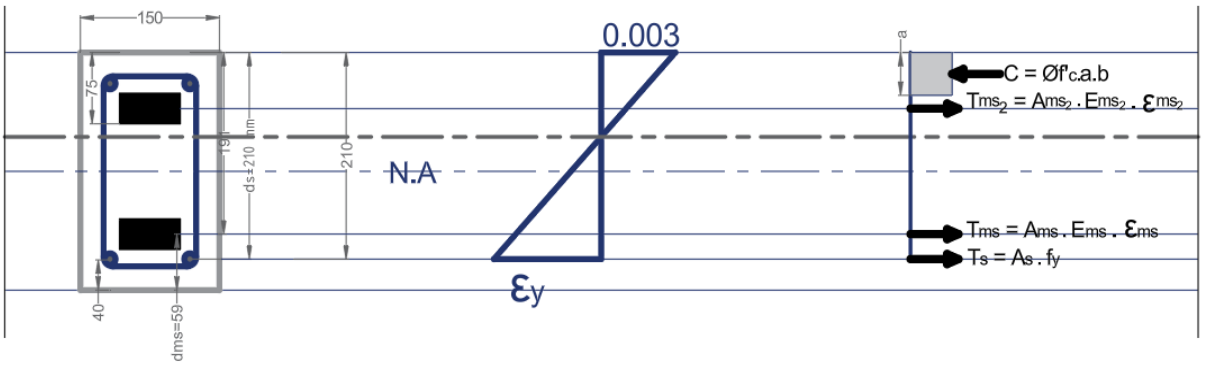

Figure 11: Compression block and tension force diagram

Table 3: Experimental and calculated load-carrying capacity.

NO.	Specimen	$P_{u\ exp.}\ (kN)$	$P_{u\ Cal}\ (kN)$	$P_{u\ Cal} / P_{u\ exp}$
1	CS	73.5	61.9	0.84
2	CFCO	72.2	61.9	0.86
3	CFSO	72.8	61.9	0.85
4	SFCOV	75.7	62.38	0.82
5	SFSOV	76.9	61.95	0.81
6	SFCOH	80.9	68.06	0.84
7	SFSOH	85.0	67.14	0.79